Removal of chlorophyll-a and microcystin-LR from spiked water using poly(ethylenediamine)-grafted mesoporous zeolite

Seung-Min Park[a], Bo-Mi Kim[a], Sangho Lee[b], Younghee Kim[c], Chan-gyu Park[a],*

[a]*Water Environmental Center, Korea Testing Laboratory, 87 Digital-ro 26-gil, Guro-gu, Seoul 08389, Republic of Korea, Tel. +82-2-860-1208; Fax: +82-2-860-1689; email: pcg6189@naver.com (C.-G. Park), jrpeter@ktl.re.kr (S.-M. Park), bmkim@ktl.re.kr (B.-M. Kim)*
[b]*School of Civil and Environmental Engineering, Kookmin University, 77 Jeongneung-ro, Jeonneung-dong Seongbuk-gu, Seoul 02707, Republic of Korea, email: sanghlee@kookmin.ac.kr*
[c]*Graduate School of Venture, Hoseo University, 2497, Nambusunhwan-ro, Seocho-gu, Seoul 06724, Republic of Korea, email: yhkim514@hoseo.com*

ABSTRACT

Harmful algal blooms (HABs) can be mitigated by employing physical, chemical, and biological control techniques to prevent eutrophication from pollution sources and restore environmental conditions. In this study, polymerized mesoporous zeolites (pMZ) were prepared by simple acid treatment and polymerization of ethylenediamine, then evaluated as adsorbents for the removal of key HAB indicators (chlorophyll-a and microcystin-LR) from aqueous solutions. The effects of treatment time on the pore structure of the pMZ were analyzed, as well as the effects of different chemical treatments during synthesis. The pMZ samples were characterized using nitrogen isotherms, X-ray fluorescence analysis, scanning electron microscopy and transmission electron microscopy image analysis, and Fourier-transform infrared spectroscopy. In order to improve the removal efficiency, amine functional groups were grafted onto mesoporous zeolite. The pMZ prepared using ammonium hexafluorosilicate had a higher mesopore volume and surface area; therefore, this method is preferred for graft polymerization. The pMZ adsorption ability was evaluated for chlorophyll-a and microcystin-LR using Langmuir, Freundlich, and Sips adsorption isotherms. The results showed that pMZ was able to remove both algae bloom indicators from an aqueous solution. Specifically, pMZ exhibited a chlorophyll-a adsorption capacity of 26.76 mg/g and removed 80% of microcystin-LR in 25 min.

Keywords: Algal bloom; Adsorption capacity; Zeolite; Graft polymerization; Chlorophyll-a

1. Introduction

Due to increasing water scarcity and water pollution control efforts around the world, the treatment of municipal and industrial wastewater has become a practical and economic method of augmenting the existing water supply, especially compared to expensive alternatives such as desalination or the development of new water sources involving dams and reservoirs [1–4]. However, wastewater treatment plants are unable to remove certain pollutants that can negatively impact humans and ecosystems [5], such as pollutants containing organic compounds that lead to eutrophication and harmful algal blooms (HABs). HABs, which are caused by excess nitrogen (N) and phosphorus (P) inputs from industrial and agricultural sources into the water, have been defined as toxic or harmful

* Corresponding author.

materials associated with microalgae that adversely affect public health, fishing activities, aquaculture, or tourism [6]. Moreover, toxic cyanobacteria of the genera *Microcystis* and *Anabaena* pose a serious problem for freshwater resources [7,8], leading to the common HAB known as blue-green algae.

In order to minimize the adverse effects of harmful algal blooms, governments and management agencies have applied various treatment methods [9,10], which can be divided into physical, physical–chemical, chemical, and biological treatments [11,12]. The magnetic separation of magnetized plankton-floc, centrifugal separation, and hypolimnetic aeration are key physical treatment methods [13,14]. Depending on the hydrodynamic characteristics, physical treatment methods may be the most practical option for controlling HABs. However, such methods are not preventative but merely control measures, and only suitable for small-scale application. Chlorides [15], copper sulfate [16], hydrogen peroxide [17], and sodium hypochlorite fulfill oxidants [18] or disinfectants [19] are common chemical treatment methods that are effective in freshwater at low concentrations. Notably, microcystin, which is considered to be hepatotoxic, is conveniently eliminated by oxidants. However, the action of four common algaecides, including copper sulfate, hydrogen peroxide, diuron, and ethyl 2-methylacetoacetate, affects the release of microcystin-LR from toxins in *Microcystis aeruginosa* [20]. Moreover, disinfection and oxidation methods are limited by their generation of by-products [21]. Biological control methods are typically environmentally friendly and employ a variety of target species, such as *Cochlodinium polykrikoides*, *Heterosigma akashiwo*, *Microcystis aeruginosa*, *M. flosauae*, *O. borgei*, and *P. globosa* [22]. However, biological treatment processes have limited treatment targets for each treatment process and are regionally limited and only suitable for water and sewage facilities. In addition, they are restricted in their direct application to lakes, dams, rivers, and seas. An alternative method consists of flocculation and subsequent sedimentation using flocculating agents [23]. In this control process, both coagulation–flocculation and sedimentation must occur. Recently, research into coagulation and adsorption has been actively conducted [24]. The method of removing algae-generating areas such as rivers and lakes is using clay or flocculant. Although it is a direct treatment method, it has the disadvantage of generating another water pollution. According to this study, the algae treatment capacity of the modified zeolite is about 0.2 L per 10 g of zeolite. The modified zeolite can be produced in a column reactor to remove algae. It has the advantage of being able to design according to the target processing capacity in the form of a column. In particular, since this study aims to remove algae on board after collecting algae from rivers or lakes, a method of removing using modified zeolite was considered. However, there are currently not many studies using modified zeolite, and commercialization and application to the field require more studies.

Since 2012, the government of the Republic of Korea has been installing dams on rivers for stream ecosystem restoration. After the implementation of these projects, HAB outbreaks increased dramatically [25]; thus, barges were employed to solve this problem. Recently, an algae removal barge has been fabricated to treat contaminated water in the Nakdong River, Korea, which employs adsorbents to rapidly remove algae in the barge [26]. In this study, novel adsorbents are prepared by using acid to transform natural zeolite into meso-zeolite. Graft polymerization is then performed to modify the surface of the meso-zeolite in order to attach a functional group. Due to the adsorption characteristics of zeolite and the electronic charge of the functional group, the resulting adsorbent can effectively remove microcystin-LR generated from *Microcystis aeruginosa* and chlorophyll-a, both of which are representative indicators of water cyanobacteria.

2. Materials and methods

2.1. Chemicals

Natural zeolite (clinoptilolite, Si/Al = 2.4, size: 3 mm) in gravel form was purchased from Geumnong Industries. 0.1 N hydrochloric acid was purchased from Samchun Pure Chemical Co., Ltd., and used without further purification. Ammonium hexafluorosilicate (AHFS) was purchased from Sigma-Aldrich (USA). The reagents used for the graft polymerization of zeolite were purchased from Sigma-Aldrich (USA); ethylenediamine (ED), sodium persulfate ($Na_2S_2O_8$), sodium metabisulfite ($Na_2S_2O_5$) 1-ethyl-3-(3-dimethylaminopropyl) carbodiimide (water-soluble carbodiimide, WSC), and N-hydroxysuccinimide (NHS) were used without further purification. Chlorophyll-a and microcystin-LR were purchased from Sigma-Aldrich (USA) and used without further purification.

2.2. Modification of mesoporous zeolite

To modify the zeolite, acid treatment was conducted then followed by AHFS treatment.

2.2.1. Dealumination zeolite with acid treatment

The natural zeolite was washed and dried at 105°C for 1 d prior to use. Then, 1 g of natural zeolite was added to 10 mL of hydrochloric acid and mixed for 1, 2, 3, 6, and 10 h at 80°C [27]. The zeolite was subsequently washed with distilled water. The remaining material was dried at 105°C for 2 h to yield mesoporous natural zeolite.

2.2.2. AHFS-treated zeolite

The solvent used for AHFS treatment was tested by altering the concentration of the solution from 1 to 20 mM. The remaining water was then removed using a vacuum distiller. The detailed experimental conditions are shown in Table 1. AHFS is typically used to reduce the amount of aluminum in zeolites [28,29]. Dealumination was performed as shown in Fig. 1. This treatment process changed the structure of the zeolite and was used to produce mesoporous zeolite (MZ).

2.3. Polymerized mesoporous zeolite

The polymerization of MZ was conducted as follows. First, 0.05 g (0.01 M) WSC and 0.1 g (0.034 M) NHS were

(a)

(b)
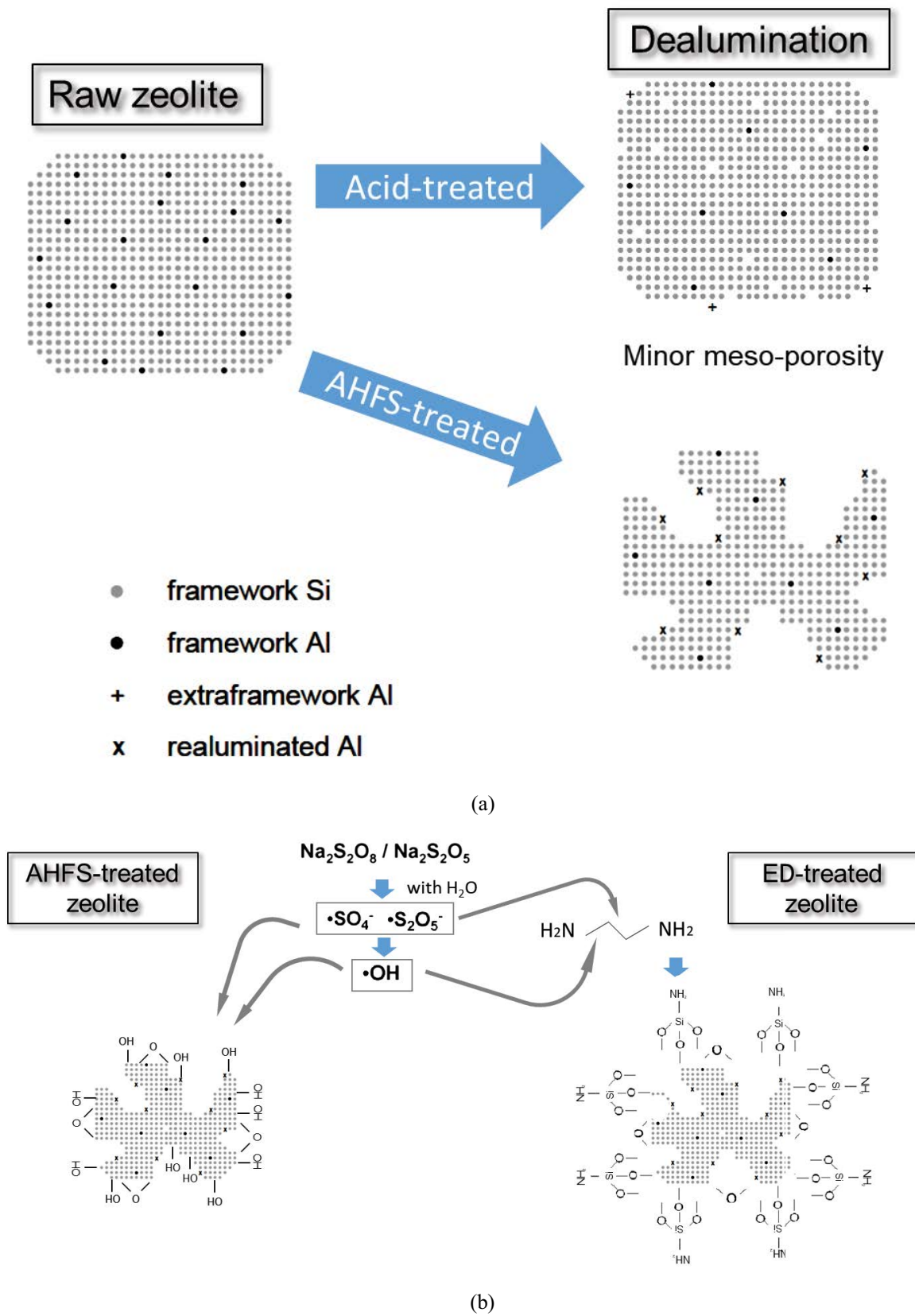
Fig. 1. Schematics of zeolite synthesis: (a) dealumination and (b) grafting polymerization.

dissolved in 10 mL DI water. Then, the solution was added to a beaker containing MZ. Ethylenediamine (40 mL, ED) was added to the beaker followed by initiators (weight ratio $S_2O_5/S_2O_8 = 0.6$). The ED, initiators, and MZ (5 g) were mixed at room temperature. After 30 min, the products were washed with deionized water. The obtained samples were denoted polymerized mesoporous zeolites (pMZ) (Fig. 1). As the zeolite post-treatment process is intended to improve the physical removal efficiency, the redox reaction improves the chemical removal efficiency. In this study, an amine group was formed on the surface of the zeolite through a redox reaction during the graft polymerization process. Physical adsorption can be combined with a secondary adsorption mechanism to improve the removal efficiency [30–32]. Such adsorption mechanisms typically include covalent and ionic bonds. The purpose of this study was to remove chlorophyll-a and microcystin-LR from water by forming positively charged amine groups.

2.4. Bach sorption studies

Adsorption isotherms are typically employed to describe the interactions and nature of the reaction between the adsorbent and the aqueous solution, which is important for designing an adsorption system. Langmuir, Freundlich, and Sips isotherm models are widely used to study adsorption processes and mechanisms. The Langmuir model is based on the hypothesis that only one layer of adsorbates are adsorbed at the adsorbent surface, where the adsorption potential is constant. The Freundlich model is an empirical application suited to highly heterogeneous surfaces, which explains multi-molecular layer adsorption at multiple homogeneous surface sites where the adsorption bonding force decreases exponentially with surface coverage [33]. The Sips model is an empirical adsorption isotherm that combines the Langmuir and Freundlich equations and is predictable over a relatively wide concentration range. Eq. (1) describes the Langmuir model [34]:

$$q_e = \frac{q_m b C_e}{1 + b C_e} \tag{1}$$

where q_e is the amount of algal organic matter adsorbed by the zeolite; C_e is the equilibrium concentration in the aqueous solution, q_{max} is the saturation capacity; K_L denotes the saturation constant. Eq. (2) describes the Freundlich model [35]:

$$q_e = K_F C_e^{1/n} \tag{2}$$

where K_F ($(mg/g)(L/mg)^{1/n}$) is the Freundlich isotherm constant and $1/n$ is the Freundlich isotherm intensity constant. The value of K_F and $1/n$ can be calculated from the intercept and the slope of the straight line of the linearized form of the Freundlich isotherm. The Sips isotherm model is obtained by introducing a power law expression on the Freundlich isotherm into the Langmuir isotherm [26]. Eq. (3) describes the Sips model [36]:

$$q_e = \frac{q_{max} K_S C_e^{1/n}}{1 + K_S C_e^{1/n}} \tag{3}$$

where K_S ($(L/mg)^{(1/n)}$) is the Sips isotherm constant, representing the energy of adsorption. The values of K_S, q_{max}, and $1/n$ can be obtained using the nonlinear regression method and the equilibrium constant related to the adsorption capacity (mg/g), the Sips maximum adsorption capacity (mg/g), and the surface heterogeneity, respectively.

2.5. Analysis method

Nitrogen (N_2) isotherms were measured at 77 K using a Micromeritics ASAP 2020 analyzer. The surface area of the sample was calculated using the Brunauer–Emmett–Teller (BET) method, and the pore size distribution was calculated using the non-local density functional theory method. The organic functional groups were characterized by attenuated total reflection–Fourier-transform infrared spectroscopy (ATR–FTIR; Nicolet 5700 spectrophotometer, Thermo Electron Corp., MA) with a ZnSe crystal at an incident angle of 45°. Sample chemistry was determined by an X-ray fluorescence (XRF) spectrometer (S4 PIONEER, Germany) installed at the NICEM at Seoul National University. The surface morphology of the zeolite was confirmed by field-emission scanning electron microscopy (FE-SEM; Hitachi S-4700). Microcystin-LR was measured using LC/MS-MS (Agilent 6460 Triple Quadrupole, USA) after pretreatment according to Environmental Protection Agency EPA Method 544.27.

3. Results

3.1. Characterization of modified zeolite

The MZ was prepared using 0.1 N hydrochloric acid (HCl) and AHFS. The materials were analyzed using N_2 adsorption–desorption isotherms, XRF, spectrometry, FTIR spectroscopy, and FE-SEM in order to confirm the order of synthesis and determine the adsorbent that exhibited the best improvement in microcystin-LR and chlorophyll-a removal compared to natural zeolite. A schematic of the overall modification procedure is shown in Fig. 1.

3.1.1. Structure of zeolite

Brunauer, Emmett, and Teller published the first paper related to the BET theory in 1938 [37], which aims to explain the mechanism of physical adsorption on a surface and forms the basis for measuring the specific surface area and pore size distribution of materials. Nitrogen isotherms were analyzed to determine the differences between the surfaces of raw zeolite (RZ), MZ, and pMZ. Nitrogen adsorption isotherms for the treated zeolite samples prepared under different synthesis conditions are shown in Table 1. The specific surface area is the most influential factor in physical removal [38,39], and was analyzed using the ASAP 2020 instrument after zeolite post-treatment (HCl and AHFS treatment). As shown in Fig. 2 and Table 2, the specific surface area increased from that of raw zeolite (449.3 m²/g) to 469.13 m²/g and 560.79 m²/g due to HCl and AHFS treatment, respectively. After HCl treatment, the micropores decreased slightly whereas the mesopores increased. After AHFS treatment, both the micropores and

mesopores increased. The surface area then decreased to 431.49 m^2/g after graft polymerization, which represented a reduction of 14.8%.

Acid treatment enabled the production of dealuminated zeolites, which is indicated by the specific surface area results. The AHFS-treated zeolites contained more mesopores than the zeolites treated with hydrochloric acid. This suggests that AHFS is more effective in generating mesoporous zeolites, which are beneficial because mesopores can increase the removal efficiency of contaminants in the water system.

3.1.2. Composition of zeolite

The Si/Al ratio was measured by XRF analysis to determine the degree of dealumination due to zeolite modification. The contents of Si and Al in raw zeolite were 56.2% and 23.4%, respectively, and the Si/Al ratio was 2.4. During acid treatment, the ratio of Si increased and the ratio of Al decreased with increasing reaction time. Therefore, the ratio of Si/Al can be increased by either increasing the concentration of HCl or increasing the reaction time. As shown in Table 3, the micropores were destroyed when the bonds between Si and Al were destroyed by acid treatment. AHFS replaces the Al bonds formed in raw zeolite by bonding with the Si functional groups. Elemental changes were not observed at low concentrations of 1 mM; however, at 20 mM, the Al content decreased

to 21.8% and the Si content increased to 65.7%, thereby increasing the Si/Al ratio.

In order to confirm the functional group structure of the zeolite, FTIR analysis was performed. Fig. 3 confirms that the Si–OH functional group increased. AHFS treatment on raw zeolites resulted in increases of 998 cm^{-1} (Si–OH (Si)), 670 cm^{-1} (Si–OH–Si), and 550 cm^{-1} (OH–Si–OH). The surface of the zeolite treated with HCl did not show any significant change [40–42].
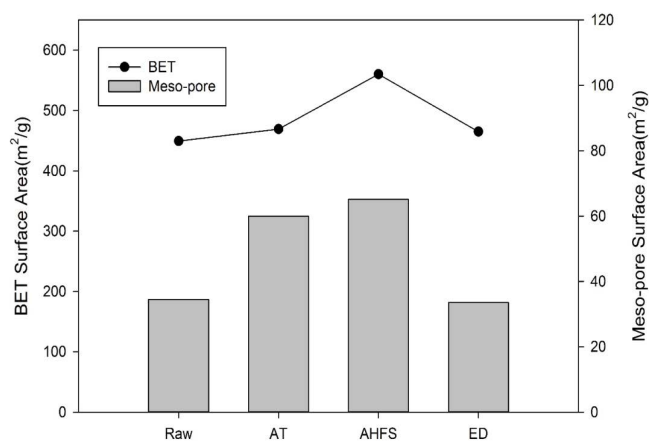
Fig. 2. Results of BET and mesopore surface area.

Table 1
Reagents and conditions for synthesis zeolite

Sorts		Naming	Temp.	Reagents	Reaction procedures	Reaction time
Raw zeolite	RZ	–	–	–	–	–
MZ	Acid treated zeolite	AT-zeolite	80°C	0.1 N HCl	1 g zeolite in 10 mL solution	1, 2, 3, 6, and 10 h
	AHFS treated zeolite	AHFS-zeolite	80°C	1, 2, 5, 10, and 20 mM ammonium hexafluorosilicate	3 g zeolite in 250 mL solution	120 min
pMZ	Grafting polymerized ED zeolite	ED-zeolite	80°C	Ethylenediamine	ED 40 mg + DI water 10 mL	15, 30, 60, and 120 min
				Water-soluble carbodiimide	• WSC 0.05 g + NHS 0.1 g	
				N-hydroxysuccinimide, sodium metabisulfite, sodium persulfate	• Na$_2$S$_2$O$_5$ 60 mg + Na$_2$S$_2$O$_8$ 40 mg	

Table 2
Results of BET analysis of zeolite

Sorts			BET surface area (m^2/g)	Micropore surface area (m^2/g)	Mesopore surface area (m^2/g)	Volume of pores (cm^3/g)
RZ	RAW	–	449.3	414.82	34.48	0.2084
MZ	AT	10 h	469.13	409.11	60.01	0.2196
	AHFS	20 mM	560.79	495.66	65.13	0.2482
pMZ	ED	15 min	465	431.49	33.51	0.2168

Table 3
Results of XRF elemental analysis. Raw is natural zeolite which untreated zeolite. AT is 0.1 N hydrochloric acid-treated zeolite according to reaction time (1, 3, 6, and 10 h). AHFS is ammonium hexafluorosilicate (AHFS) treated zeolite which is fixed reaction time (2 h) and change the concentration (1, 5, and 20 mM)

Sorts	Elements atomic (wt., %)							
	Na	Mg	Al	Si	K	Ca	Fe	Si/Al
Raw	4.7	1.8	23.4	56.2	1.71	3.55	7.42	2.4
AT-1 h	4.37	1.49	23.3	57.9	1.62	3.2	6.55	2.48
AT-3 h	4.07	1.52	23.2	57.6	1.65	3.35	6.95	2.48
AT-6 h	3.86	1.58	22.8	58.8	1.55	3.19	6.63	2.57
AT-10 h	3.25	1.55	22	59.5	1.54	3.18	6.57	2.70
AHFS-1 mM	4.23	1.52	23.5	57.4	1.62	3.42	6.92	2.44
AHFS-5 mM	4.01	1.5	23.3	57.9	1.69	3.66	6.48	2.48
AHFS-20 mM	3.63	1.46	21.8	65.7	1.54	3.46	6.95	3.01
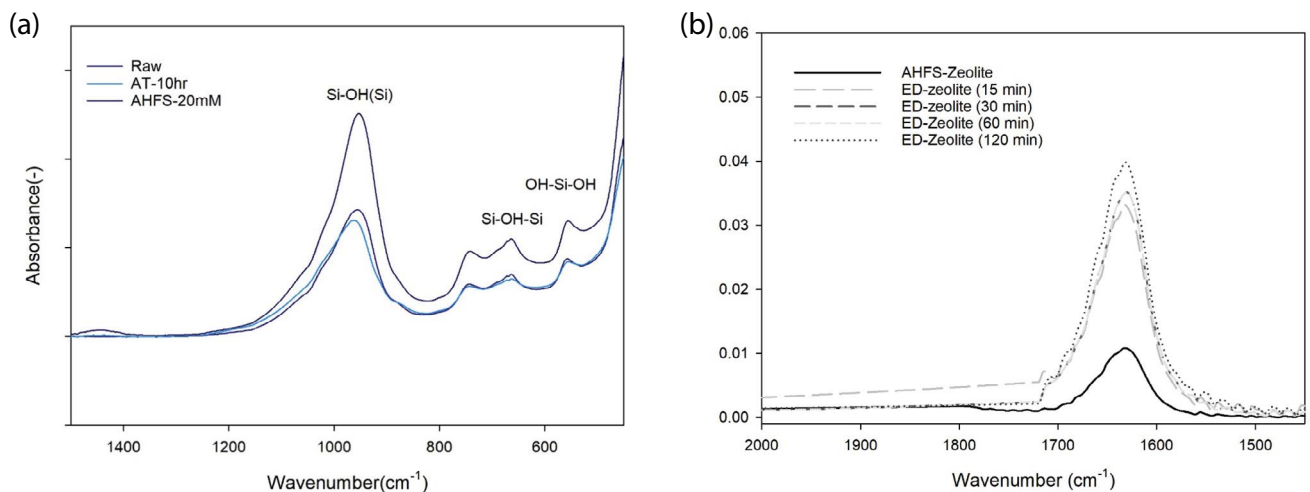
Fig. 3. ATR-FTIR spectra for (a) dealumination and (b) grafting polymerization.

The surface functional groups of the modified zeolite treated with AHFS (20 mM) were observed after graft polymerization with ED. After AHFS treatment, amide (1,660 cm^{-1}) formed on the zeolite surface due to the ED reaction [43]. It was confirmed that the chain of the amine group (amide) was longer than that of the standard zeolite due to ED-graft polymerization. Moreover, the strength of the amide increased with reaction time but not linearly; therefore, little difference was observed between 15 and 120 min. This indicates that most of the functional groups were grafted onto the surface of the zeolite within 15 min.

3.1.3. Morphology of zeolite

In order to confirm the surface changes caused by zeolite modification, the three-dimensional structure was directly observed by scanning the sample surface with an electron beam via FTIR analysis. Fig. 4 shows images of the zeolite surface at 5,000 times magnification measured at 15 kV. The zeolite before treatment exhibited a relatively homogeneous surface; however, the acid-treated zeolite and AHFS-treated zeolite exhibited increased surface roughness due to the dealumination process. In the case of ED zeolite, there was no observable difference in surface roughness from the dealuminated zeolite. Acid treatment and grafting polymerization did not result in any significant changes on the zeolite surface. Acid treatment may have altered the internal structure of the zeolite, but a minimal change in surface morphology was confirmed. Even when the surface amine group was grafted, little change was observed in the surface roughness or structure. Further research using transmission electron microscopy (TEM) images will be able to determine changes in the zeolite structure.

3.2. Adsorption isotherms

The performance of RZ, MZ, and pMZ was evaluated by isotherm experiments using 2.5 g/L of the adsorbent. Synthetic water was reacted at 25°C and 200 rpm for 5 h. The concentration was then measured and the adsorption amount was calculated using Eq. (4). Synthetic water was prepared using spiked chlorophyll-a at concentrations of 10, 20, 30, 40, 50, 70, 100, 150, 200, and 250 mg/L.
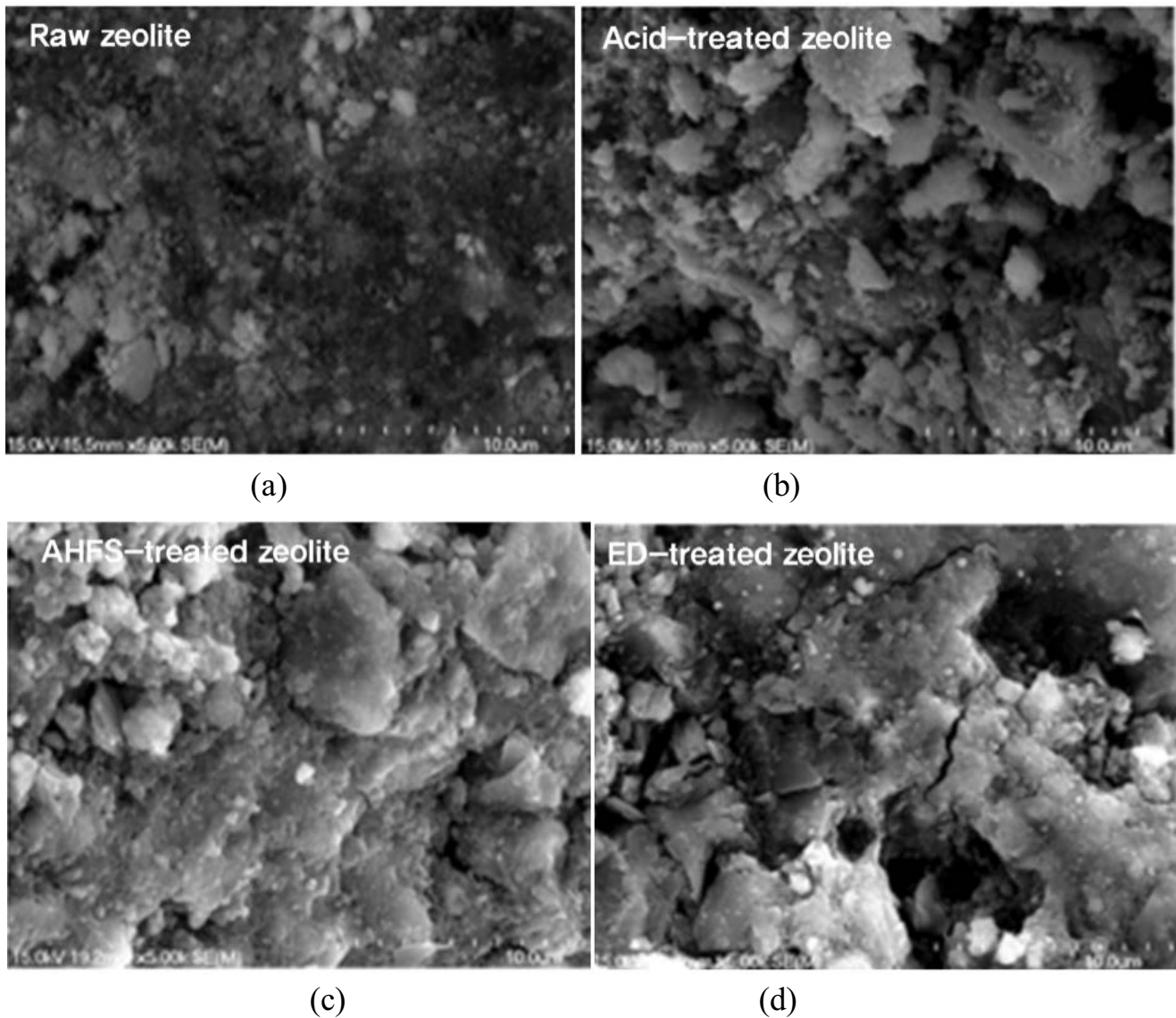
Fig. 4. FE-SEM image of mesoporous zeolite (MZ) and polymerized mesoporous zeolite (pMZ): (a) raw zeolite, (b) AT-zeolite, (c) AHFS zeolite, and (d) ED-treated zeolite.

$$q_e = \frac{(C_0 - C_e)V}{W} \tag{4}$$

where q_e is the equilibrium adsorption capacity, that is, the adsorbed amount per unit mass of zeolite (mg/g); C_0 and C_e are the initial concentration (mg/L) and equilibrium concentration (mg/L), respectively; V is the volume of the solution (L); W is the weight of the zeolite used (g). After surface modification, the removal performance of the four adsorbents was evaluated: raw zeolite (raw), acid-treated zeolite (acid), AHFS-treated zeolite, and pMZ.

In order to optimize the design of a sorption system for adsorbing chlorophyll-a from an aqueous solution, it is important to establish the most appropriate correlation for the equilibrium curves. Characterization of the adsorption process is often performed using several isotherm models. In order to evaluate the nature of adsorption, the isotherm data were analyzed using three of the most common equilibrium models, Langmuir, Freundlich, and Langmuir–Freundlich (Sips). The Langmuir model is an ideal model of more homogeneous monolayer adsorption whereas the Freundlich isotherm is more flexible and assumes that the energy of adsorption decreases logarithmically as the fractional coverage increases. The Sips model is obtained by introducing a power law expression and was created by combining the pros and cons of the Langmuir and Freundlich models.

The raw zeolite had a chlorophyll-a adsorption capacity of 2.006 mg/g (Fig. 5). The best fit values of the model parameters estimated from Eqs. (1)–(3) by nonlinear regression analysis are listed in Table 4. According to the non-linearity coefficients, R^2 and x^2, the Sips model showed a better fit than the Langmuir and Freundlich models.
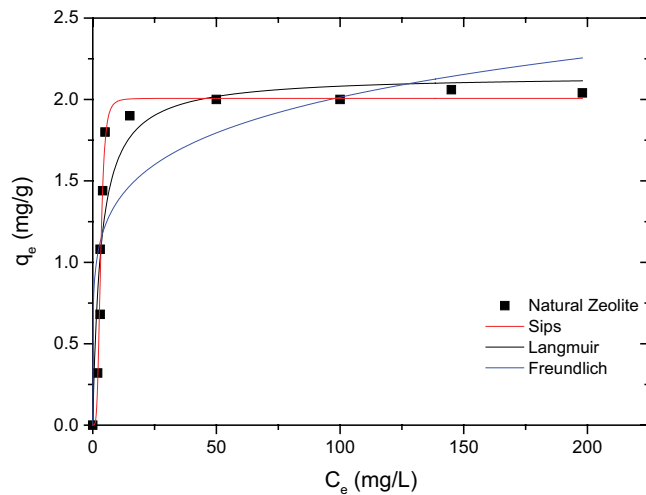
Fig. 5. Adsorption isotherm of raw zeolite.

The acid-treated zeolite showed an adsorption capacity of 4.427 mg/g (Fig. 6a), which was best fit by the Sips model. The adsorption capacities of AHFS-treated zeolite and pMZ were 21.52 and 26.76 mg/g, respectively, both of which were best fit by the Sips and Langmuir models (Figs. 6b and c). The four types of zeolite are arranged according to adsorption capacity in Table 4.

The concentration of chlorophyll-a in the test solution influenced positively the amount of adsorbed chlorophyll-a on the modified zeolites (Figs. 5 and 6). AT-zeolite and pMZ followed the Langmuir and Sips isotherm model rather than the Freundlich model implying that modified zeolite shows applicability in a wide range of contaminant concentrations. In addition Sips model indicating that the adsorption of these media is characterized by a uniform distribution of binding energies [44] obtained 0.882~0.977 of R^2 values in three modified zeolites. This result convinces the media's application and consistent efficiency in treating contaminant by adsorption.

Among the modified zeolite s, the AHFS zeolite showed the large adsorption. The dealumination treatment (AHFS zeolite) enhanced the zeolite removal efficiency the most. Through this study, zeolite pores were enlarged and functional groups were attached to the zeolite surface. In the zeolite pores, the removal mechanism acts greatly by adsorption. Functional groups, however, remove contaminants in water systems through electrical coupling. In this study, chlorophyll-a was found to be effective in adsorption.

3.3. Adsorption of toxic materials

Microcystin-LR is a toxin present in relatively large amounts in cyanobacteria. As such, it is the primary target for the removal of toxic substances from blue-green algae. To verify pMZ removal efficiency under experimental conditions of cyanotoxin contamination, the sampled waters were enriched with microcystin-LR (99% purity), then mixed and stirred for 20 min to completely dissolve the microcystin-LR prior to treatment. Removal experiments were performed using the pMZ material developed in this study. As shown in Fig. 7, 80% of the microcystin-LR was removed within 25 min.

The results of this experiment indicate that the modified zeolite can be used to remove *Microcystis*, although the removal efficiency was difficult to analyze because *Microcystis* exists in small amounts in water. The conventional process for removing *Microcystis* is oxidation, which has disadvantages such as the generation of by-products and difficulty of system configuration. It is particularly difficult to install advanced oxidation equipment on small barges. Thus, if *Microcystis* can be effectively treated with zeolites, the process of algae removal on barges will be substantially simplified.

4. Conclusions

In this study, natural zeolite was modified and used to remove blue-green algae (chlorophyll-a) and toxic substances generated from blue-green algae (microcystin-LR) from water. Natural zeolite was transformed into mesoporous zeolite through a dealumination process, which expanded the voids by removing aluminum. In addition, the zeolite pores were controlled through AHFS treatment. The AHFS-treated zeolite had a higher specific surface area than the hydrochloric acid-treated zeolite. Thus, an amine group was grafted onto the zeolite surface modified by AHFS. This synthesis method resulted in improved zeolite performance; specifically, high adsorption of chlorophyll-a and the removal of more than 80% of microcystin-LR. Thus, pMZ has substantial potential for the removal of blue-green algae, which should be further tested at the pilot scale for the simultaneous removal of blue-green algae by polymerized mesoporous zeolite.

In the Republic of Korea, there is an urgent need to control HABs that have become prevalent in rivers. In particular, HAB control technology should be appropriate for use on barges with limited capacity and volume, which are currently the best option for removing algae from rivers.

Table 4
Isotherm parameters for the adsorption of chlorophyll-a onto zeolite and modified zeolite

Sorts	Langmuir				Freundlich				Sips				
	q_m (mg/g)	B (Lm/g)	R^2	x^2	K_F	$1/n$	R^2	x^2	q_{max} (mg/g)	K_S (L/mg$^{(1/n)}$)	$1/n_s$	R^2	x^2
RZ	2.019	0.308	0.861	0.080	0.938	0.166	0.725	0.157	2.006	0.009	1.082	0.978	0.013
AT	4.641	0.159	0.975	0.071	1.131	0.298	0.885	0.331	4.427	0.128	1.239	0.977	0.0667
AHFS	22.140	0.989	0.812	11.897	11.650	0.149	0.768	14.686	21.520	0.836	4.818	0.850	9.476
ED	26.76	1.034	0.895	10.673	14.089	0.147	0.876	12.596	26.56	1.049	1.151	0.882	12.002
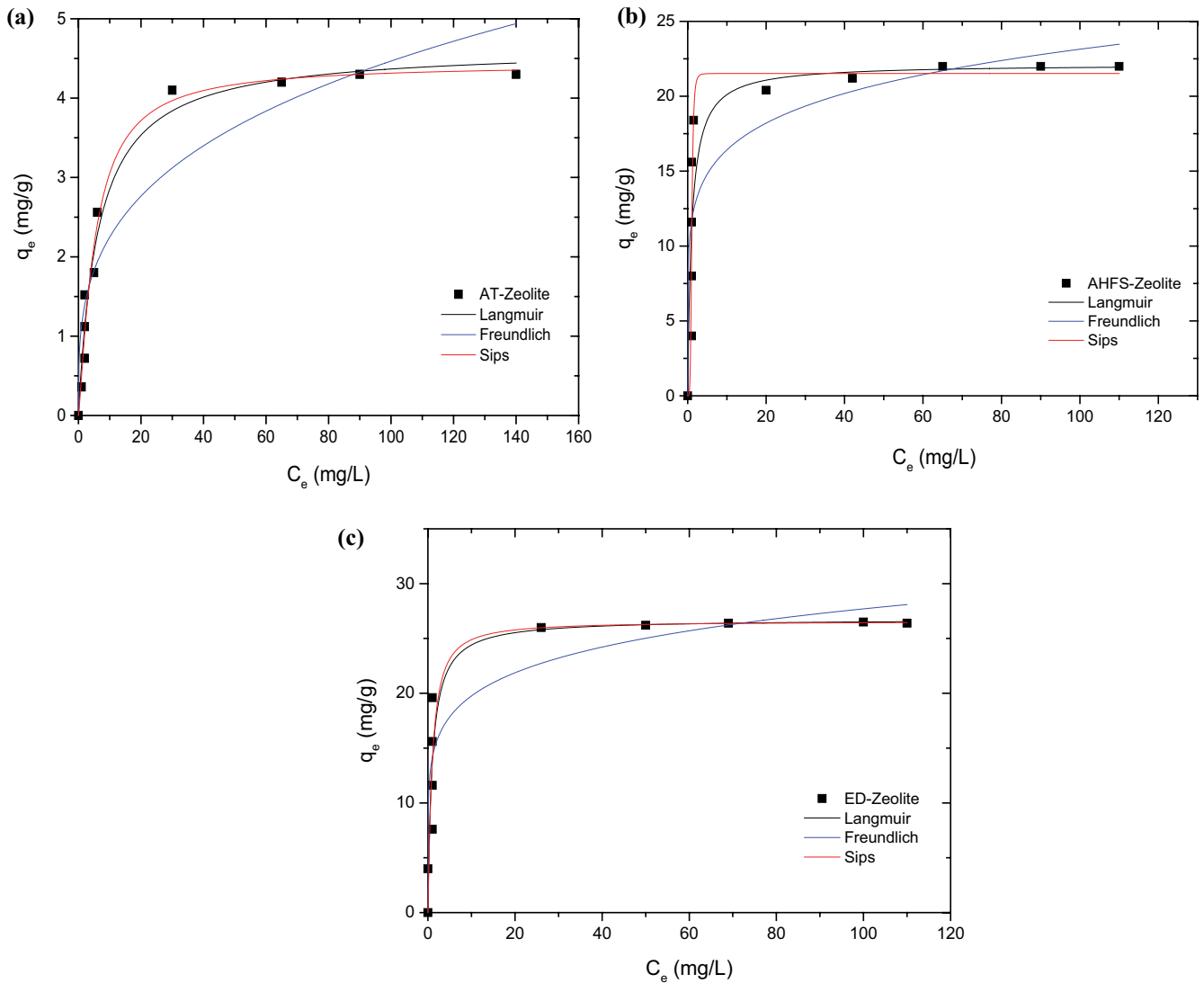
Fig. 6. Adsorption isotherm of mesoporous zeolite (MZ): (a) AT-zeolite, (b) AHFS-zeolite, and (c) polymerized mesoporous zeolite (pMZ).

Therefore, the treatment method proposed in this study will not only protect the river ecosystem but also reduce the social costs of HAB response measures.
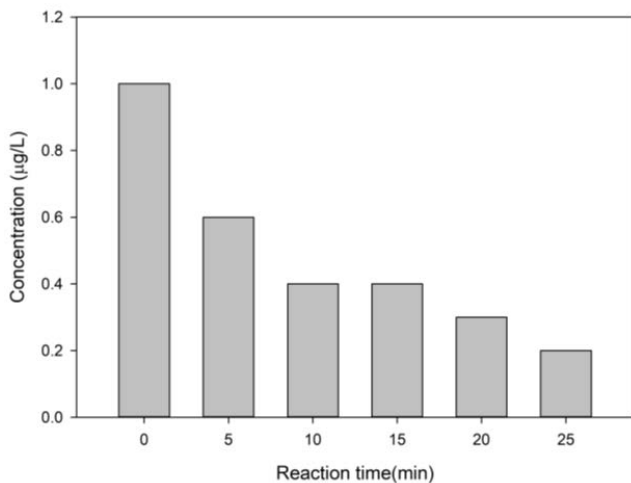
Fig. 7. The removal efficiency of microcystin-LR using pMZ.

References

[1] R. Costanza, R. d'Arge, R. de Groot, S. Farber, M. Grasso, B. Hannon, K. Limburg, S. Naeem, R.V. O'Neill, J. Paruelo, R.G. Raskin, P. Sutton, M. van den Belt, The value of the world's ecosystem services and natural capital, Nature, 387 (1997) 253–260.
[2] R.G. Luthy, Bioterrorism and water security, Environ. Sci. Technol., 36 (2002) 123A.

[3] K.R. Zodrow, Q.L. Li, R.M. Buono, W. Chen, G. Daigger, L. Dueñas-Osorio, M. Elimelech, X. Huang, G.B. Jiang, J.-H. Kim, B.E. Logan, D.L. Sedlak, P. Westerhoff, P.J.J. Alvarez, Advanced materials, technologies, and complex systems analyses: emerging opportunities to enhance urban water security, Environ. Sci. Technol., 51 (2017) 10274–10281.

[4] J.B. Rose, Viewpoint: water quality security, Environ. Sci. Technol., 36 (2002) 246A–250A.

[5] I. Chorus, J. Bartram, Toxic Cyanobacterial in Water: A Guide to Their Public Health Consequences, Monitoring and Management, St. Edmundsbury Press Ltd., London, New York, 1999.

[6] K.G. Sellner, G.J. Doucette, G.J. Kirkpatrick, Harmful algal blooms: causes, impacts and detection, J. Ind. Microbiol. Biotechnol., 30 (2003) 383–406.

[7] M. Scheffer, S. Carpenter, J.A. Foley, C. Folke, B. Walker, Catastrophic shifts in ecosystems, Nature, 413 (2001) 591–596.

[8] L. Guo, Doing battle with the green monster of Taihu Lake, Science, 317 (2007) 1166.

[9] M. Lürling, F. van Oosterhout, Controlling eutrophication by combined bloom precipitation and sediment phosphorus inactivation, Water Res., 47 (2013) 6527–6537.

[10] M. Robb, B. Greenop, Z. Goss, G. Douglas, J. Adeney, Application of Phoslock™, an innovative phosphorus binding clay, to two Western Australian waterways: preliminary findings, Hydrobiologia, 494 (2003) 237–243.

[11] E. Zohdi, M. Abbaspour, Harmful algal blooms (red tide): a review of causes, impacts and approaches to monitoring and prediction, Int. J. Environ. Sci. Technol., 16 (2019) 1789–1806.

[12] J.J. Gallardo-Rodríguez, A. Astuya-Villalón, A. Llanos-Rivera, V. Avello-Fontalba, V. Ulloa-Jofré, A critical review on control methods for harmful algal blooms, Rev. Aquacult., 11 (2019) 661–684.

[13] X.F. Kang, M.J. Zhou, Y. Fukuyo, O. Matsuda, S.-G. Lee, H.-G. Kim, V. Shulkin, T. Orlova, Eds., Booklet of Countermeasures Against Harmful Algal Blooms (HABs) in the NOWPAP Region, NOWPAP Special Monitoring and Coastal Environmental Assessment Regional Activity Centre (NOWPAP CEARAC), 5–5 Ushijimashin-machi, Toyama 930–0856, Japan, 2007, p. 243.

[14] M.R. Sengco, D.M. Anderson, Controlling harmful algal blooms through clay flocculation, J. Eukaryotic Microbiol., 51 (2004) 169–172.

[15] R. Renner, T. Eichenseher, L. Thrall, Quick, cheap method for algae removal, Environ. Sci. Technol., 40 (2006) 1377.

[16] Z. Wang, S.Y. Lu, D.Y. Wu, F. Chen, Control of internal phosphorus loading in eutrophic lakes using lanthanum-modified zeolite, Chem. Eng. J., 327 (2017) 505–513.

[17] I. de Vicente, P. Huang, F.Ø. Andersen, H.S. Jensen, Phosphate adsorption by fresh and aged aluminum hydroxide. Consequences for lake restoration, Environ. Sci. Technol., 42 (2008) 6650–6655.

[18] X.-C. Chen, H.-N. Kong, S.-B. He, D.-Y. Wu, C.-J. Li, X.-C. Huang, Reducing harmful algae in raw water by light-shading, Process Biochem., 44 (2009) 357–360.

[19] A. Kleeberg, C. Herzog, M. Hupfer, Redox sensitivity of iron in phosphorus binding does not impede lake restoration, Water Res., 47 (2013) 1491–1502.

[20] S.Q. Zhou, Y.S. Shao, N.Y. Gao, Y. Deng, J.L. Qiao, H. Ou, J. Deng, Effects of different algaecides on the photosynthetic capacity, cell integrity and microcystin-LR release of *Microcystis aeruginosa*, Sci. Total Environ., 463–464 (2013) 111–119.

[21] D.M. Anderson, Approaches to monitoring, control and management of harmful algal blooms (HABs), Ocean Coastal Manage., 52 (2009) 342.

[22] W.W. Carmichael, Health effects of toxin-producing cyanobacteria: "The CyanoHABs", Hum. Ecol. Risk Assess.: Int. J., 7 (2001) 1393–1407.

[23] J. Berkowitz, M.A. Anderson, C. Amrhein, Influence of aging on phosphorus sorption to alum floc in lake water, Water Res., 40 (2006) 911–916.

[24] A.J.H. Pieterse, A. Cloot, Algal cells and coagulation, flocculation and sedimentation processes, Water Sci. Technol., 36 (1997) 111–118.

[25] J.Y. Kim, T. Lee, D. Seo, Algal bloom prediction of the lower Han River, Korea using the EFDC hydrodynamic and water quality model, Ecol. Modell., 366 (2017) 27–36.

[26] S.W. Jung, H. Cho, D.H. Kim, K.W. Kim, J.-I. Han, H. Myung, Development of algal bloom removal system using unmanned aerial vehicle and surface vehicle, IEEE Access, 5 (2017) 22166–22176.

[27] D.M. Roberge, H. Hausmann, W.F. Hölderich, Dealumination of zeolite beta by acid leaching: a new insight with two-dimensional multi-quantum and cross polarization ^{27}Al MAS NMR, Phys. Chem. Chem. Phys., 4 (2002) 3128–3135.

[28] M.-C. Silaghi, C. Chizallet, J. Sauer, P. Raybaud, Dealumination mechanisms of zeolites and extra-framework aluminum confinement, J. Catal., 339 (2016) 242–255.

[29] M. Ibáñez, E. Epelde, A.T. Aguayo, A.G. Gayubo, J. Bilbao, P. Castaño, Selective dealumination of HZSM-5 zeolite boosts propylene by modifying 1-butene cracking pathway, Appl. Catal., A, 543 (2017) 1–9.

[30] P. Loganathan, S. Vigneswaran, J. Kandasamy, Enhanced removal of nitrate from water using surface modification of adsorbents – a review, J. Environ. Manage., 131 (2013) 363–374.

[31] G.J. Ehlert, Y.R. Lin, H.A. Sodano, Carboxyl functionalization of carbon fibers through a grafting reaction that preserves fiber tensile strength, Carbon, 49 (2011) 4246–4255.

[32] A.S. Sarac, Redox polymerization, Prog. Polym. Sci., 24 (1999) 1149–1204.

[33] T.S. Anirudhan, P. Senan, Adsorption characteristics of cytochrome C onto cationic Langmuir monolayers of sulfonated poly(glycidylmethacrylate)-grafted cellulose: mass transfer analysis, isotherm modeling and thermodynamics, Chem. Eng. J., 168 (2011) 678–690.

[34] I. Langmuir, The adsorption of gases on plane surfaces of glass, mica and platinum, J. Am. Chem. Soc., 40 (1918) 1361–1403.

[35] H.M.F. Freundlich, Over the adsorption in solution, J. Phys. Chem., 57 (1906) 385–471.

[36] R. Sips, On the structure of a catalyst surface, J. Phys. Chem., 16 (1948) 490–495.

[37] S. Brunauer, P.H. Emmett, E. Teller, Adsorption of gases in multimolecular layers, J. Am. Chem. Soc., 60 (1938) 309–319.

[38] G.N. Okolo, R.C. Everson, H.W.J.P. Neomagus, M.J. Roberts, R. Sakurovs, Comparing the porosity and surface areas of coal as measured by gas adsorption, mercury intrusion and SAXS techniques, Fuel, 141 (2015) 293–304.

[39] C. Scherdel, G. Reichenauer, M. Wiener, Relationship between pore volumes and surface areas derived from the evaluation of N$_2$-sorption data by DR-, BET- and t-plot, Microporous Mesoporous Mater., 132 (2010) 572–575.

[40] L. Bokobza, Spectroscopic techniques for the characterization of polymer nanocomposites: a review, Polymers (Basel), 10 (2018) 7, https://doi.org/10.3390/polym10010007.

[41] W.H. Zhou, E.L. Clennan, Relative reactivities of tethered functional groups in the interior of a zeolite, Org. Lett., 2 (2000) 437–440.

[42] X. Rao, M. Tatoulian, C. Guyon, S. Ognier, C.L. Chu, A. Abou Hassan, A comparison study of functional groups (Amine vs. Thiol) for immobilizing AuNPs on zeolite surface, Nanomaterials (Basel), 9 (2019) 1034, doi: 10.3390/nano9071034.

[43] J.-H. Kim, P.-K. Park, C.-H. Lee, H.-H. Kwon, Surface modification of nanofiltration membranes to improve the removal of organic micro-pollutants (EDCs and PhACs) in drinking water treatment: graft polymerization and cross-linking followed by functional group substitution, J. Membr. Sci., 321 (2008) 190–198.

[44] S.X. Duan, X.T. Xu, X. Liu, J. Sun, T. Hayat, A. Alsaedi, J.X. Li, Effect of Fe$_3$O$_4$@PDA morphology on the U(VI) entrapment from aqueous solution, Appl. Surf. Sci., 448 (2018) 297–308.